Excitation Energy Transfer in Ion Pairs of Polymethine Cyanine Dyes: Efficiency and Dynamics

G. Ponterini,[†] M. Fiorini,[†] D. Vanossi,[†] A. S. Tatikolov,[‡] and F. Momicchioli*,[†]

Dipartimento di Chimica, Università di Modena e Reggio Emilia and INSTM, Via Campi 183, I-41100 Modena, Italy and Institute of Chemical Physics, Academy of Sciences of Russia, Kosygin Street 4, Moscow, Russia

Received: January 2, 2006; In Final Form: March 23, 2006

The present work deals with singlet excitation energy transfer (EET) occurring in contact ion pairs (CIPs) of several anionic oxonol analogues (acting as EE donors) and cationic cyanines (acting as acceptors) characterized by *off resonance* individual transitions. Combining conductometric and spectroscopic measurements with decreasing solvent polarity, we were able to observe a progressive ion pairing leading first to solvent-separated ion pairs (SSIPs) and then to CIPs. Analysis of the absorption spectra of three selected salts (A2,C1, A2,C2, and A1,C4) in chloroform−toluene mixtures showed that the transformation of SSIP into CIP involves the appearance of a certain exciton coupling, the extent of which decreases regularly with increasing gap between the local excitation energies. Fluorescence excitation spectra showed that EET occurs in CIP, and EET efficiencies were evaluated with a procedure expressly devised for weakly emitting donors. These were between 0.2 and 0.65 for the examined ion pairs involving anions A1 and A2. The spectroscopic study was complemented by a theoretical investigation aimed at establishing the dynamic regime of the observed EET. From classical MD simulations and local full geometry optimizations, A2,C1 and A2,C2 were found to form rather stable sandwich-type CIP structures with interchromophore distances (R) of about 0.45−0.50 nm. The donor−acceptor electronic coupling was calculated in terms of Coulombic interactions between atomic transition charges. For CIP, the electronic coupling was decidedly beyond the limit of the weak coupling required for an incoherent Förster-type mechanism. Thus, we tried to arrange the EET dynamics within the theory developed by Kimura, Kakitani, and Yamato (*J. Phys. Chem. B* **2000**, *104*, 9276) for the intermediate coupling case, which provides analytical expressions of time-dependent occupation probability, EET rate, and coherency in terms of two basic quantities: the electronic coupling and a correlation time related to the Franck−Condon factor. The latter was shown to be primarily modulated by Förster's spectral overlap integral (related in turn to the excitation energy gap). Calculations were carried out for the three sample systems using three values of the electronic coupling roughly corresponding to CIP, 1.0, and 2.0 nm interchromophore distances. At the CIP distance, EET in both A2,C1 and A2,C2 was predicted to occur with a partial exciton mechanism, very short transfer times (about 10 fs), and high degree of coherence. In A1,C4 (having the largest energy gap), EET was found to occur with a hot-transfer mechanism. More or less hot-transfer dynamics appeared to be retained by all three systems at $R = 1.0$ nm. Fully incoherent EET appeared to become operative only at distances larger than 2.0 nm.

1. Introduction

The study of light-induced phenomena in organized assemblies of cyanine dyes is important in view of the wide use of such systems for photonic and sensing technologies.[1] Usually, practical applications require stacking of cyanine chromophores within solid structures, like Langmuir−Blodgett[2] or self-assembled[3] films. On the other hand, self-association phenomena occurring in homogeneous solution can be driven to form a variety of dye aggregates (homodimers, heterodimers, H and J aggregates) that are suitable for basic studies on the processes promoted by interactions between electronically excited chromophores, ranging from exciton coupling (EC) to excitation energy transfer (EET) and light-induced electron transfer (ET). Starting from previous extensive studies on solution photochemistry and electronic spectra of cyanines and merocyanines[4] (and references therein), we adopted this stratagem to investigate the structural, spectroscopic, and photophysical properties of dimers and ion pairs (heterodimers) formed in solutions of ionic cyanines under selected conditions.[5−7] Scheme 1 provides a general picture of the various association types that may occur in solutions of salts formed by a cationic (C) and an anionic (A) cyanine upon changing the solvent characteristics.

Briefly, in aqueous solution, a progressive increase of concentration yields H-dimerization of the dissociated monomers, followed by the formation of higher H- and J-aggregates. Such processes are induced essentially by dispersion and hydrophobic forces. As is well-known, the formation of these species is evidenced by sharp modifications of the absorption spectra (relative to those of the monomers) describable in the frame of the coherent exciton model.[8,9] In refs 5 and 6, the effects of dimerization on the spectroscopic and photophysical properties of some anionic oxacarbocyanines (with colorless

* To whom correspondence should be addressed. Tel: 0039 59 2055081. Fax: 0039 59 373543. E-mail: momicchioli.fabio@unimore.it.
[†] Università di Modena e Reggio Emilia.
[‡] Academy of Sciences of Moscow.

10.1021/jp0600211 CCC: $33.50
Published on Web 06/01/2006

SCHEME 1

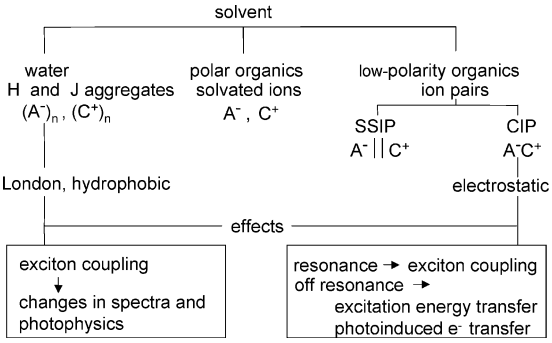

counterions) were investigated experimentally, and the theoretical bases of the observed behavior were settled by molecular dynamics (MD) calculations of the dimer structure and CS INDO CI comparative study of the monomer and dimer spectra.

Coming back to Scheme 1, a progressive decrease of the solvent polarity will lead in turn to the formation of solvated ions, solvent-separated ion pairs (SSIPs), and contact ion pairs (CIPs). The latter species (heterodimers) may in principle give rise to different light-induced phenomena according to the relative values of two main parameters:[10,11] (i) the interaction energy between the electronic states of the AC complex involving S_0-S_1 excitation at A and C, $V_{AC} = \langle A^*C|\hat{V}|AC^*\rangle$, and (ii) the difference between the S_0-S_1 transition energies of A and C (ΔE_{exc}), controlling the spectral overlap of their lowest-energy absorption bands. In this connection, however, CIPs of cyanine dyes hold a special position since the high S_0-S_1 transition moment of the individual chromophores and the rather small interchromophore distance (see later and ref 7) make the value of V_{AC} to be invariably high. So, the light-induced behavior is primarily governed by the ΔE_{exc} value.

In the small ΔE_{exc} limit, where the S_0-S_1 transitions of the two components are in *resonance* (Scheme 1), the CIP will feature a behavior similar to that of the homodimers. In short, because of the strong coupling, the excitation will delocalize over the two components, thus generating two new (well-separated) electronic states described by exciton theory as due to transitions to the in-phase and out-of-phase combinations of the locally excited states.[8,9] In ref 7, we analyzed in detail this coupling range by an experimental and theoretical study on CIP formed by cyanine and oxonol dyes featuring almost superimposed color bands. The observed spectroscopic and photophysical behavior was shown to be traceable to a predominant presence of ion pairs characterized by parallelism of both the long molecular axes and the molecular planes.

On the other hand, if the S_0-S_1 excitations of the two components are *off resonance*, namely, their absorption regions are sufficiently far apart, then the fit conditions may take place for a "localized" excitation at one of the components (acting as the *donor*, D) followed by EET or ET to the other (*acceptor*, A) (Scheme 1). The present work is concerned with mechanism and dynamics of EET in a series of DA CIPs formed by proper combinations of five oxonol-like anions (all based on the heptamethine primary chromophore) with five cyanine cations including three thiacarbocyanine derivatives (C1, C2, C2(ET)), pinacyanol (C3), and thiadicarbocyanine (C4) (Scheme 2).

The subject was undertaken from both an experimental and a theoretical point of view. In the experimental part, we report conductometric and spectroscopic evidence for the formation of SSIPs and CIPs upon changing from polar to low polarity and from low polarity to almost nonpolar solvents. It is shown, in particular, that, at ΔE_{exc} values comparable with the average width of the absorption bands of the two components, the formation of CIPs gives rise to appreciable modifications of the spectrum attributable to partial, yet significant, exciton delocalization. We then report the EET efficiencies (r_{EET}) determined by a steady-state approach expressly devised for donor/acceptor pairs characterized by very weakly fluorescent donors, such as those of the ion pairs under study (Scheme 2). Finally, the r_{EET} values obtained in toluene−chloroform mixtures of different composition are discussed in reference to the corresponding variations of the fluorescence excitation spectra.

In an attempt to go beyond the information obtained by the steady-state spectroscopy, we carried out a theoretical study aimed at gaining an insight into the dynamics of interchromophore EET in the ion pairs investigated. Precisely, we intended to position the dynamic regime between the limit cases of the strong coupling (coherent EET) and the very weak coupling (incoherent EET).[10−12] The investigation was focused on the (A2,C1) and (A2,C2) pairs in view of their relatively small ΔE_{exc} (2500−3000 cm^{-1}) suggesting that they may fit into the case of the intermediate coupling (partially coherent EET).[13,14] As a first step, we searched for realistic structures of the CIP combining MD simulations using a classical force field[15] and local full geometry optimizations at the PM3 (third parametric method) level.[16] The study was then addressed to the calculation of the donor−acceptor electronic coupling $V_{DA} = \langle D^*A|\hat{V}|DA^*\rangle$ based on CS INDO CI[17] descriptions of the locally excited states, already tested in previous theoretical investigations about EC and EET in molecular aggregates.[18−21] In keeping with the above qualitative considerations, the V_{DA} values obtained for contact (A2,C1) and (A2,C2) pairs (R_{eq} = 4.5/5 Å) were found to be beyond the weak coupling limit. The degree of coherence was estimated within the theory of the EET rate developed by Kimura, Kakitani, and Yamato[14] for the intermediate coupling case. It turned out that, for the ion pairs investigated, interchromophore separations of >20Å are required so that the EET dynamics may follow a Golden-rule-type rate equation.[22] Extension of the analysis to (A1,C4), exhibiting a ΔE_{exc} value appreciably greater than the bandwidths of the separated chromophores, has shown that even in this case the EET mechanism appears to retain a nonnegligible degree of coherence.

2. Experimental Study

2.1. Materials and Instrumentation. All dye salts employed in this study were obtained from the collection of Zh. A. Krasnaya (Institute of Organic Chemistry, Russian Academy of Sciences, Moscow, Russia) and were used without further purification. Solvents were of spectroscopic grade. Samples were stored in the dark so as to minimize photodegradation. Absorption and fluorescence excitation spectra were frequently rechecked to make sure that solutions were acceptably stable in the time scale necessary for measurements, that is, some tens of minutes. For fluorescence excitation measurements, maximum absorbances were kept between 0.05 and 0.1.

Absorption spectra were measured with a Perkin-Elmer Lambda-15 spectrophotometer. Fluorescence spectra were obtained from a Jobin Yvon-Spex FluoroMax-2 spectrofluorometer. Excitation spectra were corrected for the instrumental spectral response using a self-made correction curve, checked with several different fluorescent dyes between 420 and 660 nm.

2.2. Ion Pairing and Interchromophore Interaction. Dissolution of salts occurs with the formation of species roughly categorized as free ions, contact ion pairs (CIPs), and solvent-

SCHEME 2

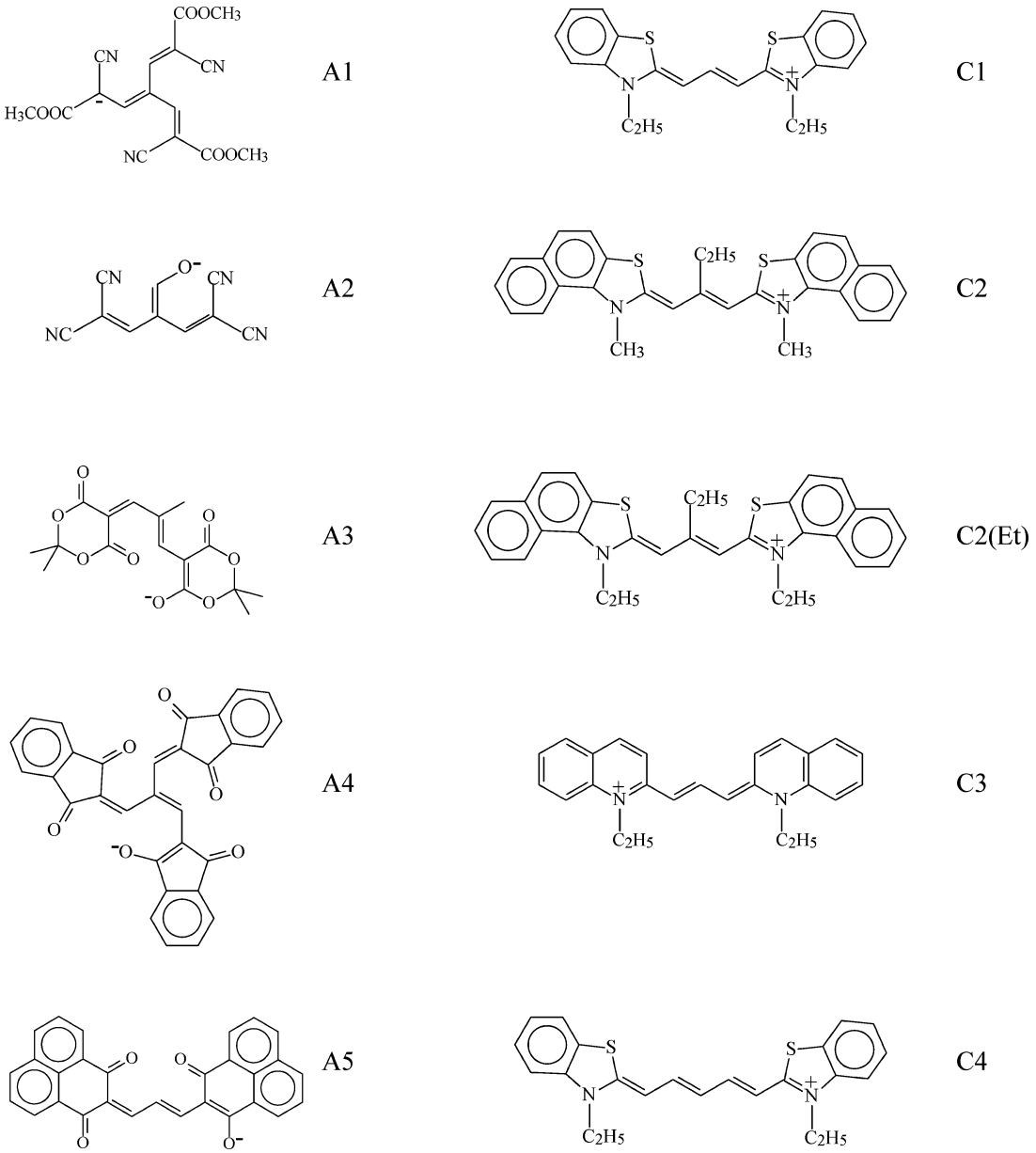

TABLE 1: Electrical Conductivities (χ, 30 °C) and Wavelengths of Absorption Maxima (λ_{abs}^{max}) of A2,C1 Solutions (6×10^{-6} M)

solvent	CH_3OH	CH_3CN	$(CH_3)_2CO$	CH_2Cl_2	$CHCl_3$	1:1 $CHCl_3$−toluene	toluene
ϵ	32.7	37.5	20.7	8.9	4.8		2.4
χ (μS cm^{-1})	2.4	1.4	0.8	0.55	0.15	0	0
λ_{abs}^{max} (nm)	476, 556.5	488, 554.5	518, 557	520, 562	519, 565	495, 569	498, 574

separated (including solvent-shared) ion pairs (SSIPs).[23] The existence of chemically distinguishable types of ion pairs was experimentally demonstrated long ago (see ref 24 for a review of this early work) and was later supported by a large number of computer simulations (for some representative studies, see refs 25−29). In the following, our ion pairing observations are discussed within this general framework.

First of all, electrical conductivity data of A2,C1 (Table 1) clearly indicate a progressive association in ion pairs upon moving to solvents of decreasing polarity. In particular, in chloroform, the salt is almost completely associated and becomes fully so in a 1:1 chloroform−toluene mixture. The absorption band of the cationic cyanine C1 exhibits a weak negative solvatochromism (second figure in the corresponding line of Table 1). Similarly, the band of the anionic dye A2 shifts bathochromically upon moving from methanol to acetonitrile to acetone. In this solvent, as well as in dichloromethane and chloroform, however, the band merges with the first vibronic shoulder of C1 and a single maximum is observed whose wavelength is reported in Table 1.

It is well established that the CIP/SSIP interconversion equilibrium is shifted toward SSIP as a good solvating medium (usually an organic solvent of intermediate-to-high polarity) is added to a solution of a salt in an associating solvent (typically, hydrocarbons and some ethers).[30,31] Indeed, when we move from chloroform to toluene, through binary mixtures of variable composition, the absorption spectra of A2,C1 change in a fashion different from that expected from the mentioned negative

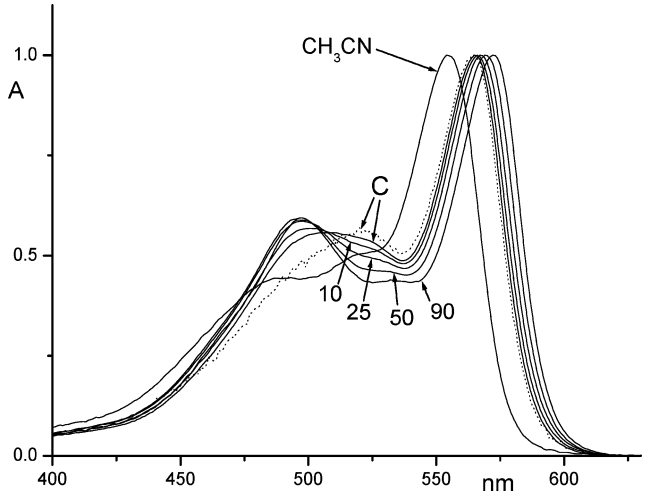

Figure 1. Absorption spectra of A2,C1 in acetonitrile and chloroform-(C)−toluene mixtures (figures indicate the percent fraction of toluene). All spectra were normalized at the C1 maximum. Sample concentrations were about 3×10^{-6} M (full line) and 3×10^{-7} M (dotted line).

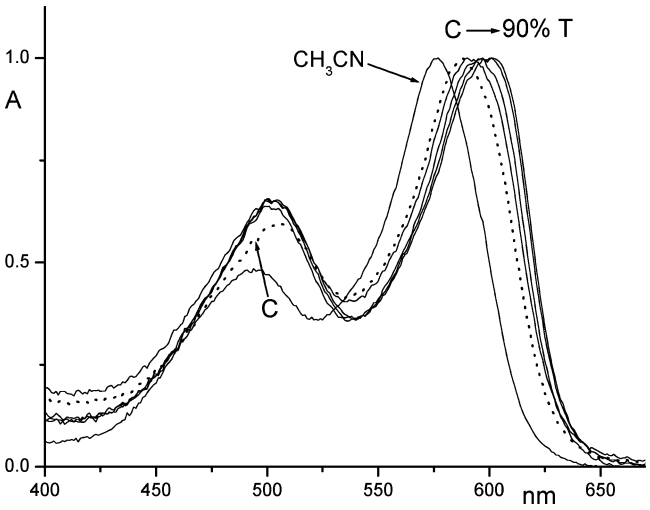

Figure 2. Normalized absorption spectra of A2,C2 in acetonitrile, chloroform (C), and C−toluene (T) mixtures with 25, 50, 80, and 90% T. Sample concentrations were about 5×10^{-7} M.

solvatochromism (Figure 1). While the absorption band of C1 keeps shifting bathochromically, with increasing toluene content in the mixture, the A2 absorption band separates from the vibronic shoulder of C1 undergoing a slight hypsochromic shift (maximum around 498 nm) at low amounts of toluene and becomes better and better pronounced in toluene-richer mixtures. Since the fraction of CIPs relative to those of SSIPs and solvated ions is expected to increase along the binary mixture series, we attribute the anomalous spectral behavior to partial exciton interaction occurring in the A2,C1 CIP. Indeed, the phenomenon depends on the total concentration in chloroform: the CIP band increases with concentration (compare the two spectra in chloroform in Figure 1). The whole spectral modification associated with formation of CIP is better appreciated comparing the spectrum in a 90% toluene mixture with that in acetonitrile (Figure 1). Interestingly, such an effect was weaker for salt A2,C2 (Figure 2): here, the maximum of the absorption band of A2 moves from about 505 nm in chloroform to about 500 nm in chloroform−toluene mixtures, with no significant change in band shape. To explain this behavior, let us consider the two main differences between A2,C2 and A2,C1. First of all A2,C2 is characterized by a slightly larger difference between the

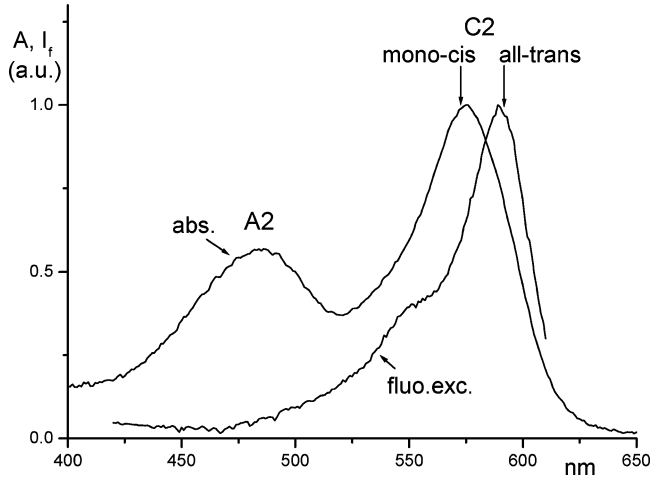

Figure 3. Normalized absorption and corrected fluorescence excitation spectra of A2,C2 in acetonitrile. The monitoring wavelength was 620 nm. Sample concentrations were about 5×10^{-7} M.

excitation energies (ΔE_{exc}) of the anionic and cationic chromophores. Second, the two cations have a structurally important difference: while C1 has no substituent in the polymethine chain, C2 bears an ethyl group in the meso position. Because of steric hindrance of this with the two S atoms, the all-trans isomer (which is the only species present in C1 solutions) is destabilized relative to the cis one obtained by twisting about a central C−C bond. So, a mixture of the two isomers can be observed in solutions of C2. This was reported in pioneering literature on thiacyanines[32,33] and a more recent contribution on the photophysics of meso-substituted thiacarbocyanines.[34] It is confirmed by the noncoincidence of the absorption and fluorescence excitation spectra in acetonitrile (Figure 3): consistently with the cited literature,[33] we observe emission mainly from the all-trans isomer, which is known to absorb bathochromically relative to the mono-cis one.[35] On the other hand, a study carried out in ref 32 on the stereoisomerism of a similar compound (3,3′-diethyl-9-methylthiacarbocyanine), showed that the isomeric all-trans/mono-cis equilibrium shifts decidedly toward the all-trans component upon moving from methanol to toluene solutions. Thus, we can reasonably assume that the formation of the A2,C2 CIP in low-polarity solvents involves preferably the all-trans form of C2 and that, consequently, the weaker spectral modifications observed for A2,C2 in toluene-rich solutions are essentially due to the slightly larger ΔE_{exc} giving rise to a reduced exciton interaction. Indeed, comparison between the spectrum in 90% toluene solution and that in acetonitrile (Figure 2) shows that, apart from a marked negative solvatochromism of the C2 absorption, the spectral effect associated with formation of CIPs consists essentially in an increased relative intensity in the region of the A2 absorption.

The relation between ΔE_{exc} and spectral modifications induced by exciton coupling is further clarified by Figure 4 showing the absorption spectra in different solvents of A1,C4, which is characterized by the largest ΔE_{exc} among the ion pairs considered in this study (see the next section).

Clearly, the red shift of the absorption maximum of C4 upon moving from acetonitrile ($\lambda_{max} = 650$ nm) to chloroform ($\lambda_{max} = 667$ nm) can be entirely attributed to the solvatochromic effect. The further red shift observed upon moving from chloroform to toluene ($\lambda_{max} = 678$ nm) might be partly due to exciton coupling in the CIPs formed in this associating solvent. Now, the quasi-coincidence of λ_{max} of C4, observed with such a nonchromophoric counterion as I^- in toluene solution ($\lambda_{max} = 679$ nm), points to a minor role of the exciton interaction in

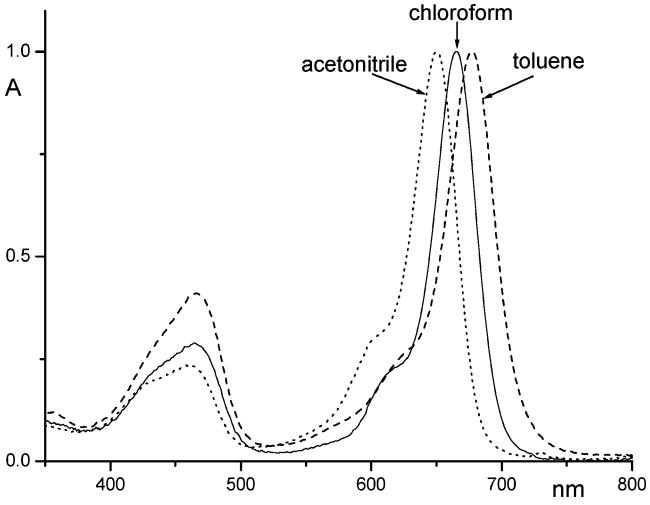

Figure 4. Normalized absorption spectra of A1,C4 in three different solvents. Sample concentrations were about 5×10^{-7} M.

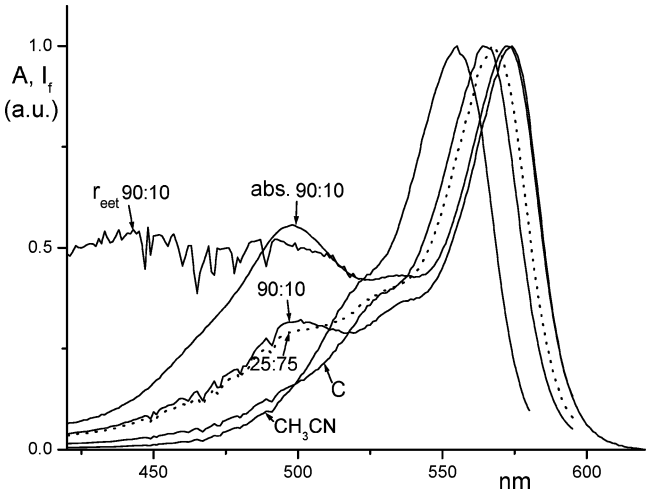

Figure 5. Normalized absorption (abs) and corrected fluorescence excitation spectra of A2,C1 in acetonitrile, chloroform (C), and some toluene−chloroform mixtures (volume fractions reported). Monitoring wavelengths were 590 (acetonitrile) and 605 nm. r_{EET} is the EET efficiency estimated with eq 5 in the Appendix.

the CIP of A1,C4. On the other hand, the sizable increase in the relative intensity of the A1 absorption ($\lambda_{max} \approx 460$ nm) upon moving from chloroform to toluene is indicative of at least a feeble exciton interaction.

In summary, although the spectral changes associated with CIP formation are much less pronounced than in "resonant" ion pairs,[7] the spectral evolutions showed in Figures 1, 2, and 4 can be taken as evidence of the occurrence of a certain interion exciton coupling in the (A2,C1), (A2,C2), and (A1,C4) CIPs. The size of such moderate coupling is expected to undergo a progressive decrease, upon moving from A2,C1 to A2,C2 to A1,C4, connected with a corresponding increase of ΔE_{exc}. Later on, we will show that such not very marked differences may be enough to cause sensibly different EET dynamics in these ion pairs.

2.3. EET in Ion Pairs. Evidence of the occurrence of EET in A2,C1 and A2,C2 CIP is shown in Figures 5 and 6. In both cases, the excitation spectra of the EE acceptors (C1 and C2) show no contributions from the donor A2 in a dissociating solvent such as acetonitrile. On the contrary, such contributions begin to appear in chloroform and rapidly attain their maximum

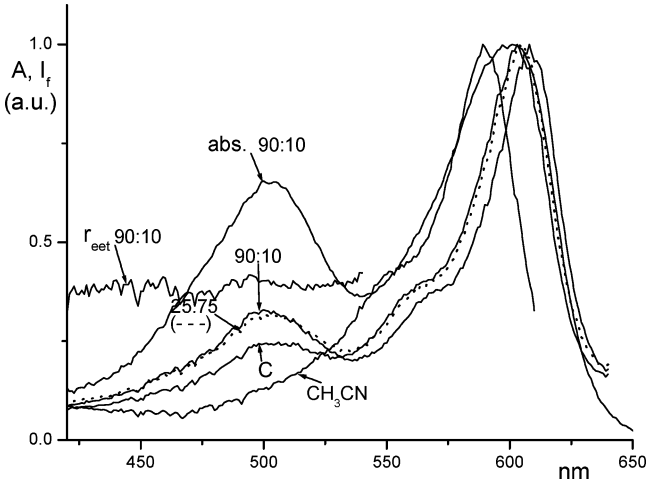

Figure 6. Normalized absorption (abs) and corrected fluorescence excitation spectra of A2,C2 in acetonitrile, chloroform (C), and some toluene−chloroform mixtures (volume fractions reported). Monitoring wavelengths were 620 (acetonitrile) and 650 nm. r_{EET}, the efficiency of EET, was estimated through eq 4 in the Appendix.

TABLE 2: Excitation-energy Differences (ΔE_{exc}) between Anion and Cation in CH_3CN and EET Efficiencies (r_{EET}) of Various Donor (anion)/Acceptor (cation) Pairs in Chloroform (C) and in a 9:1 Toluene−Chloroform Mixture (TC)[a]

anion	cation	ΔE_{exc}/eV	r_{EET} in C	r_{EET} in TC
A1 (460, 0.83)	C2 (576, 1.70)	0.54	0.22	0.30
A1	C2(Et) (576)	0.54	0.22	0.30
A1	C3 (604, 1.18)	0.64	0.35	0.65
A1	C4 (651, 1.37)	0.79	0.05	0.20
A2 (480, 0.77)	C1 (555, 1.09)	0.35	0.10	0.45
A2	C2	0.43	0.25	0.40
A3 (468, 0.99)	C4	0.74	0.02	0.05
A4 (545, 1.16)	C4	0.37	∼0	∼0
A5 (561, 1.30)	C4	0.31	∼0	∼0

[a] Maximum absorption wavelengths (nm) and oscillator strengths in acetonitrile are given within parentheses. Sample concentrations were between 4 and 8×10^{-7} M.

values in chloroform−toluene mixtures with increasing fraction of the latter associating solvent. Quantification of these observations is provided by the values of the efficiency of EET (r_{EET}) determined by the procedure described in the Appendix. The r_{EET} values were found to increase from chloroform to chloroform−toluene mixtures, reaching their maximum values already at low toluene fractions (compare the 25:75 and the 90:10 normalized excitation spectra in Figures 5 and 6). This suggests that, in keeping with the very low solubilities of these salts in toluene, the CIPs are already dominant in toluene-poor binary mixtures.

We observed an analogous behavior with several other salts (see Table 2 and Scheme 2). To briefly go through the results, we may safely assume that a shift of the equilibria, favoring SSIP vs solvated ions and CIP vs SSIP, takes place as we move from chloroform to mixtures with an increasing fraction of toluene. Indeed, the EET efficiency increases regularly, though not always by the same factor, upon moving from chloroform to the 9:1 toluene−chloroform mixture. Its value, in the nonresonant donor/acceptor pairs investigated, spans a fairly large range, from 0 to 0.65. It should be emphasized that, because of the coupled equilibria involving solvated ions, SSIP and CIP in solutions of these dyes and the likely different equilibrium constants, the fractions of CIP vs SSIP and solvated

ions may be different from sample to sample, despite the similar total concentrations. This prevents a strict, quantitative comparison of r_{EET} values from being carried out. On the whole, we may say that a cation based on the thiadicarbocyanine chromophore such as C4 seems to be a worse EET acceptor than those carrying shorter chromophores such as thiacarbocyanine (C1, C2, and C2(Et)) and pinacyanol (C3). However, this criterion based on the difference in the excitation energies of the anion and the cation (ΔE_{exc} in Table 2) cannot alone explain the very low values of r_{EET} in ion pairs of anions A4 and A5 with C4, since here the differences in absorption maxima between the donor and the acceptor are comparable with those found in the cases where EET is efficient. So, we are forced to look for other possible explanations. First, we rule out the possibility that such salts do not associate in ion pairs in the 9:1 toluene−chloroform mixture, since electrical conductivities were essentially zero for solutions at concentrations of the order of 10^{-5} M. Then, we notice that EET appears to be more efficient in ion pairs of anions A1 and A2 which are slightly more compact and less bulky than the other three. This may allow for the formation of more intimate CIPs where EET may be more efficient. Somewhat contrary to this hypothetical explanation, however, r_{EET} is consistently larger for these ion pairs in chloroform too, where SSIPs, having much looser structures than CIPs, are supposed to be present in larger amounts than in toluene (evidence of this was given above for A2,C1). Finally, it is worth recalling that quantum efficiencies are balance parameters which express the competitiveness of a decay route vs the other ones. So, the low values found for anions A3−A5 relative to A1 and A2 may simply reflect the fact that other excited-state decay channels are faster in the former than in the latter cases.

3. Theoretical Study

3.1. Methodologies and Calculations. The computational working plan encompassed both ground-state structures and excited-state properties of separated ions as well as of ion pairs. The calculation series and the procedures adopted in each case are outlined below. Here, we point out that, following previous theoretical studies on structures and spectra of dimers and ion pairs of cyanine dyes,[5,7] all calculations were made in the absence of solvent. Such a simplification was assumed to be qualitatively acceptable considering that EET occurs in ion pairs lying inside a cage of a "nonpolar" solvent.

3.1.1. Ground-State Structures of Ions and Ion Pairs. Structure calculations were performed by previously described procedures[5,7] using the HyperChem computational package.[15] Briefly, the individual ion structures were calculated by full geometry optimization at the PM3 level,[16] while ion-pair structures were derived by a two-step procedure involving (i) localization of the more stable configuration by MD simulation adopting the classical MM+ force field[15] and (ii) structure refinement by local geometry optimization at the PM3 level.

3.1.2. V_{DA} Electronic Matrix Element. The calculation of the donor−acceptor electronic coupling promoting EET in ion pairs was approached within the exciton approximation,[18−21] that is, assuming that the excited-state wave functions of the isolated chromophores remain unperturbed by the interchromophore interactions. In this scheme, the V_{DA} integral is given by

$$V_{DA} = \langle D^*A|\hat{V}|DA^*\rangle \qquad (1)$$

Where $|D^*A\rangle$ and $|DA^*\rangle$ are ion-pair wave functions representing localized excitations at D and A, respectively, and $\hat{V}$ is the interchromophore Coulombic operator. Detailed analyses of the V_{DA} matrix element are available in the literature[36,37] (and references therein). Here, we simply recall that the total electronic coupling can be written as

$$V_{DA} = V_{DA}^{Coul} + V_{DA}^{short} \qquad (2)$$

where V_{DA}^{Coul} is the Coulombic term and V_{DA}^{short} is the short-range term including penetration (V_{DA}^{pen}) and electron-exchange (V_{DA}^{exch}) interactions due to interchromophore orbital overlap. In our case, where strongly allowed $S_0 \rightarrow S_1$ transitions on D and A are involved, V_{DA}^{Coul} is expected to predominate over V_{DA}^{short}, even at small interchromophore separations. As a matter of fact, detailed calculations of V_{DA}^{exch} using the Mulliken approximation for two-electron repulsion integrals showed that $V_{DA}^{Coul}/V_{DA}^{exch} \geq 10^5$ at the interchromophore separations occurring in CIPs (4.5−5 Å).[38] Most likely, the same holds true for the V_{DA}^{pen} term having the same intermolecular overlap dependence as V_{DA}^{exch}.[36] Thus, we can legitimately assume that $V_{DA} \cong V_{DA}^{Coul}$ for the singlet−singlet energy transfer considered here.

Following a procedure extensively used in previous studies of exciton coupling,[18−21,39] the Coulombic interaction term was first approximated as the sum of the electrostatic interactions between the atomic transition charges of D and A associated with their individual $S_0 \rightarrow S_1$ excitations

$$V_{DA}(R^{-1}) = \sum_{d\in D}^{N_D}\sum_{a\in A}^{N_A} \frac{q_d q_a}{R_{da}} \qquad (3)$$

where N_D (N_A) is the number of atoms of D (A), q_d (q_a) is the atomic transition charge of the atom d ∈ D (a ∈ A), and R_{da} is the distance between the centers of atoms d and a.

Second, V_{DA} was obtained by direct calculation within the NDO approximation. This way, V_{DA} turns out to be simply given by

$$V_{DA}(\gamma) = \sum_{d\in D}^{N_D}\sum_{a\in A}^{N_A} q_d q_a \gamma_{da} \qquad (4)$$

Where γ_{da} are the (interchromophore) two-center Coulombic integrals and the other symbols have the same meaning as those in eq 3. With atomic transition charges being the same, eqs 3 and 4 differ from one another only in that the former considers simple electrostatic interactions between point charges located at the centers of the atoms, while the latter is based on effective charge−charge interactions depending on what γ_{da} integrals are adopted. In general, $V_{DA}(\gamma) < V_{DA}(R^{-1})$ but their difference vanishes at large interchromophore separations since $\gamma_{da} \rightarrow R_{da}^{-1}$ in the limit $R_{da} \rightarrow \infty$.

The atomic transition charges entering eqs 3 and 4 were obtained by carrying out CS INDO CI calculations[17] for the individual ions. An outline of the CS INDO method and the parametrization details can be found in ref 7 (and references therein). We only point out that in the present work intrachromophore γ integrals were parametrized according to Ohno−Klopman (OK)[40] and that CI calculations included a few singly excited configurations (SCI) of the $\pi\pi^*$ type. Precisely, the SCI was expanded on a limited basis of three highest occupied and three lowest virtual π MOs. Such a limited CI is consistent with the fact that the S_1 donor and acceptor excited states involved in EET can be described fairly well in terms of the only (HOMO,LUMO) configuration. For the calculation of $V_{DA}(\gamma)$

(eq 4), the so-obtained transition charges were combined with different interchromophore γ_{da} integrals calculated according to OK[40] and MN[41] formulas as well as using Slater atomic orbitals.

3.1.3. EET Rate Expressions. The donor−acceptor electronic coupling (V_{DA}) evaluated by the procedures described above was used to estimate the dynamic regime of the observed EET processes.

For the EET rate constant in the limit of the weak coupling ($V_{DA} \ll \Delta E_{exc}$), we refer to a Golden-rule expression given by[10,22]

$$k_{DA}^{GR} = V_{DA}{}^2 \frac{9(\ln 10)10^{-9}}{128\pi^5 N_A \tau_r^D} \left(\frac{4\pi\epsilon_0}{|\mathbf{M}^D||\mathbf{M}^A|}\right)^2 J_{DA} \qquad (5)$$

where N_A is Avogadro's constant, τ_r^D is the donor radiative lifetime, ϵ_0 is the vacuum permittivity, $|\mathbf{M}^D|$ and $|\mathbf{M}^A|$ are the donor and acceptor dipole transition moments, and J_{DA} is a spectral overlap integral given by

$$J_{DA} = \int_0^\infty f_D(\lambda)\epsilon_A(\lambda)\lambda^4 \, d\lambda \qquad (6)$$

where $f_D(\lambda)$ is the normalized fluorescence spectrum of the donor and $\epsilon_A(\lambda)$ is the molar absorption coefficient of the acceptor.[42] All the quantities on the right-hand side of eq 5 need to be expressed in SI units, except for J_{DA} which has to be given in M^{-1} cm^3. Equation 5 may be applied on condition that vibrational relaxation at the photoexcited state of donor is faster than energy transfer. This establishes an upper limit for the incoherent EET rate ($k_{DA} \leq 10^{12}$ s^{-1}) that in our case may take place only for large interchromophore distances (small V_{DA}) and/or large ΔE_{exc} (small J_{DA}).

However, the conditions for incoherent EET are hardly fulfilled by the CIPs considered in the present study. This requires application of theories capable of covering the whole range of the EET dynamic regimes. We followed the nonperturbative theory developed by Kimura et al.[14] for a three-state model[43] consisting of the ground state of the donor plus a photon ($D + h\nu$) as the initial state ($|d\rangle$), the excited state of the donor D* as the intermediate state ($|m\rangle$), and the excited state of the acceptor A* as the final state ($|a\rangle$). Solution of the quantum Liouville equation for this three-state system (see ref 14 for all details) led to an analytical formula for the probability that the system exists in the final state $|a\rangle$ at time t after absorbing a photon, given by

$$n_a(t) = 1 - e^{-t/\tau_c}\left[\cosh(\sqrt{\alpha}t) + \frac{\sinh(\sqrt{\alpha}t)}{2\tau_c\sqrt{\alpha}}\right]^2$$

$$\alpha = \frac{1}{4\tau_c{}^2} - \frac{V_{DA}{}^2}{\hbar^2} \qquad (7)$$

where τ_c is the correlation time for the two-time correlation function of the excitation transfer interaction, which was assumed to decrease exponentially with time.[44] This correlation time was shown to be proportional to the Franck−Condon overlap between the intermediate state $|m\rangle$ and the final state $|a\rangle$ ($\tau_c = \pi\hbar$(FC), eq 34 in ref 14). On the basis of the value of V_{AD}, Kimura et al. fixed criteria to distinguish among coherent (exciton), intermediate, and incoherent (Förster-type) dynamic regimes. Qualitatively speaking, for $V_{DA} \gg \hbar/2\tau_c$, that is, $\alpha < 0$, $n_a(t)$ is an oscillatory function reflecting a fast EET back and forth between donor and acceptor (exciton mechanism). On the other hand, in the limit $V_{DA} \ll \hbar/2\tau_c$, that is, $\alpha > 0$, $n_a(t)$ will evolve according to a Golden-rule-type mechanism. Within these limits (intermediate coupling), Kimura et al. distinguish two types of dynamic regimes: (i) partial exciton, where the oscillatory coherent character is partly retained and (ii) hot transfer, where the oscillatory character is no longer retained but EET sets out before the vibrational relaxation at the photoexcited donor is completed.

Equation 7 leads to a time-dependent rate $k_{ad}(t) = dn_a(t)/dt$ expressed as follows[14]

$$k_{ad}(t) = \frac{V_{DA}{}^2}{\hbar^2} e^{-t/\tau_c}\left\{1 + \frac{\tanh(\sqrt{\alpha}t)}{2\tau_c\sqrt{\alpha}}\right\} \frac{\tanh(\sqrt{\alpha}t)}{\sqrt{\alpha}\,(1 - \tanh^2(\sqrt{\alpha}t))} \qquad (8)$$

An EET rate expression suitable for all of the dynamic regimes was then defined as

$$k_{ad}^{max} = \left.\frac{dn_a(t)}{dt}\right|_{t=t\max} = k_{ad}(t_{max}) \qquad (9)$$

where t_{max} is the time when the slope of $n_a(t)$ becomes maximum. In the oscillatory case, k_{ad}^{max} is taken equal to the first maximum slope. The so-defined k_{ad}^{max} corresponds to the Golden-rule rate in the weak coupling case and equals $V_{DA}/\hbar$ in the fully resonant case. Proper expressions of t_{max} for $\alpha > 0$ and $\alpha < 0$ derived under the condition of the maximum slope of $n_a(t)$[45] allow k_{ad}^{max} to be calculated (eq 8) for all values of V_{DA} (provided that τ_c has been evaluated).

Finally, Kimura et al.[14] found that the degree of coherence (or simply coherency) η of any specific EET process can be expressed analytically as

$$\eta = 1 - \frac{\sqrt{1 + C} - Ct_{max}/\tau_c}{1 - C}, \quad \text{where } C = 4V_{DA}{}^2\tau_c{}^2/\hbar^2 \qquad (10)$$

For $C \gg 1$ (strong coupling limit) and $C \ll 1$ (weak coupling limit), η becomes 1 and 0, respectively. The special point $C = 1$, where $\alpha = 0$ or $V_{DA} = \hbar/2\tau_c$, corresponds to the critical coherency $\eta_c = \lim_{C\to 1} \eta = 1 - (2)^{1/2}/3 = 0.528595...$ which represents the middle point in the intermediate coupling region.

As is evident from the foregoing presentation, practical calculation of $n_a(t)$, k_{ad}^{max}, and η for the V_{DA} values peculiar to the heterodimers under study (CIP) requires the correlation time (τ_c) to have been determined. In ref 14, concerned with EET in homodimers and heterodimers of bacteriochlorophyls, τ_c was obtained by estimation of the Franck−Condon factor between the $|m\rangle$ and $|a\rangle$ states (FC) and the equation $\tau_c = \pi\hbar$(FC). To limit the degree of arbitrariness inherent in the current estimations of the FC factors, in the present work, τ_c was determined by an alternative procedure based on the fact that in the limit of the very weak electronic coupling k_{ad}^{max} reduces to the Golden-rule EET rate constant (k_{DA}^{GR}). Now, from eq 8 ($t = t_{max}$), it turns out that as $V_{DA} \to 0$ (say $\alpha \to 1/4\tau_c{}^2$) $k_{ad}^{max} \to \tau_c V_{DA}{}^2/\hbar^2$, so that by substitution into eq 5 we have

$$\tau_c = \hbar^2 \frac{9(\ln 10)10^{-9}}{128\pi^5 N_A \tau_r{}^D} \left(\frac{4\pi\epsilon_0}{|\mathbf{M}^D||\mathbf{M}^A|}\right)^2 J_{DA} \qquad (11)$$

which makes it possible to evaluate τ_c using absorption and emission data of the isolated components. Equation 11 is in

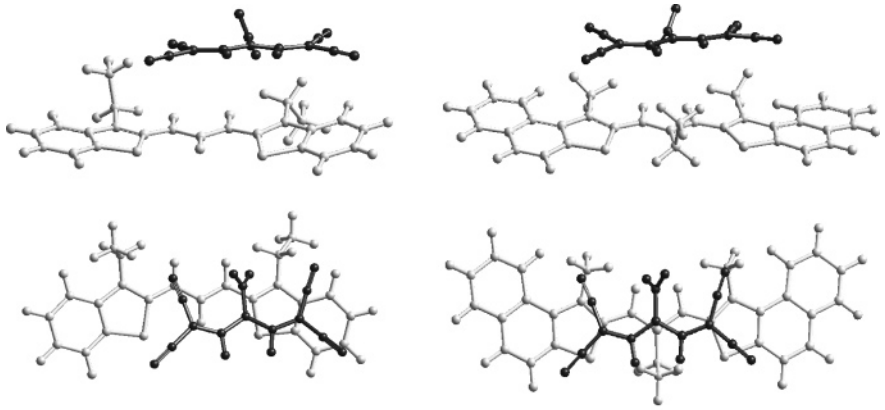

Figure 7. Structures of the A2,C1 and A2,C2 CIPs. The bottom and top representations emphasize the almost parallel arrangements of the long molecular axes and the molecular planes, respectively.

keeping with eq 34 of ref 14, since it expresses the proportionality of τ_c to the Franck−Condon overlap between the *equilibrium* $|m\rangle$ state and the $|a\rangle$ state (see eq 6.11 in ref 22). In the present study, the so-estimated correlation time, $\tau_c(\infty)$, was assumed to be the same as the correlation time for the Franck−Condon $|m\rangle$ state, $\tau_c(0)$.

3.2. Results and Discussion. In concert with the experimental investigation presented in the previous section, the theoretical study was primarily focused on the ion pairs formed by anion A2 with cations C1 and C2. This choice seemed to us to be quite significant since the A2,C1 and A2,C2 pairs have the smallest ΔE_{exc} among the CIPs exhibiting high r_{EET} (Table 2). Therefore, in accordance with a certain degree of exciton coupling evidenced by the spectra (section 2.2), in such systems, the EET is expected to take place with partially coherent or hot-transfer mechanisms. Through the use of reasonable values of the electronic coupling, in section 3.2.3 the theoretical analysis will be extended to the A1,C4 system which is characterized by the largest ΔE_{exc} among the ion pairs experimentally investigated (Table 2).

3.2.1. Ground-State Structures of Individual Ions and Ion Pairs. The search for reasonable structures was carried out assuming that A2, C1 e C2 have an all-trans configuration at the central polymethine chain and that such a configuration is retained in the formation of the heterodimers A2,C1 and A2,C2. This assumption, quite reliable for A2 and C1, was extended to C2 on the basis of the considerations made in section 2.2 on the structure of the meso-substituted thiacarbocyanines in low-polarity solvents. Local full geometry (PM3) optimizations at the all-trans configurations yielded quasi-planar structures except for the Me and Et groups of C1,C2 and the −CHO group of A2 oriented perpendicularly to the plane of the chromophoric system. As expected for symmetric cyanines, the C−C bonds of the central polymethine chains were found to have similar lengths around 1.40 Å.

Starting from all-trans configurations of the monomers, MD simulations and local full geometry optimizations yielded two types of stable ion-pair structures differing primarily for the "parallel" or "perpendicular" arrangement of the chromophore long axes. In both A2,C1 and A2,C2 ion pairs, the structure with perpendicular arrangement was found to be slightly less stable (∼10 kJ mol^{-1}), so for conciseness, the theoretical study was focused on the parallel-type structures shown in Figure 7. The main characteristics of the structures in Figure 7 can be summarized as follows: (i) the two components retain almost the same geometries as those obtained for the isolated ions, (ii) the molecular planes of the two chromophores are nearly parallel (as are the long molecular axes), and (iii) the average distances between the molecular planes are ∼4.8 Å for A2,C1 and ∼4.4 Å for A2,C2.

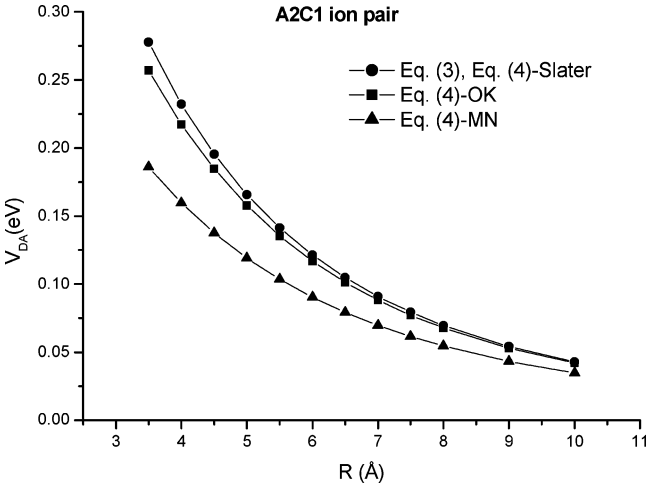

Figure 8. Variation of the electronic coupling with interchromophore distance, *R*, for the donor and acceptor S_1 states of the A2,C1 ion pair. The effects of using different recipes for Coulombic interchromophore interactions are shown (for the meaning of the symbols, see the text).

The interion interaction energy, calculated (at the PM3 level) as the difference between the energy of the CIP and that of the separate ions, turned out to be ∼ −210 kJ mol^{-1} for both systems. As pointed out in ref 7 for similar CIPs, such a value is indicative of a considerable stability mainly due to the electrostatic interaction between the oppositely charged ions.

3.2.2. Electronic Coupling. This section reports an analysis of the interaction matrix element V_{DA} describing the coupling between the singlet excited states (S_1) of the donor (A2) and the acceptor (C1 or C2) involved in the EET. V_{DA} was calculated by eqs 3 and 4 using the D and A atomic transition charges obtained by the above-described CS INDO SCI treatment of the individual ions (section 3.1.2). The study was centered on the determination of the distance-dependence of the coupling strength. For this purpose, standard ion-pair arrangements similar to those of Figure 7 were first built up using the optimized structures of the separate ions and V_{DA} was then calculated at 12 values of the distance (*R*) between the planes of the chromophores in the interval 3.5−10 Å. Figure 8 shows the results obtained for A2,C1 using four different approximations for the interchromophore two-center Coulombic interactions.

Quite similar values of V_{DA}, omitted here for brevity, were obtained for the A2,C2 ion pair at all interchromophore distances. This may be partly due to shortcomings of the calculation procedure as, for example, a too limited CI. However, qualitatively speaking, this result is quite reasonable considering that the two acceptors C1 and C2 share the pentamethine cyanine chromophore (Scheme 2) on which the respective S_0-S_1 excitations are (more or less) localized. Thus, appreciably different $S_1(D)-S_1(A)$ coupling strengths might be induced only by marked differences in the ion-pair structures, which were left out in the present study.

As to the three curves in Figure 8, we comment as follows. Of course, all curves converge at large interchromophore separations since they have to conform to the simple dipolar approximation when the donor−acceptor distance becomes much larger than the molecular dimensions. Around the equilibrium distances (4.5−5.0 Å), the different recipes for the interchromophore Coulombic interactions lead to appreciably different couplings. The highest values were obtained using the point charge approximation (eq 3) or γ_{da} integrals calculated with Slater atomic orbitals. The two choices appear to be practically equivalent in the entire explored interval of interchromophore distances. Use of OK γ_{da} integrals provided V_{DA} values a little smaller than the point-charge ones, while rather smaller values were obtained adopting the MN integrals. The mean values of V_{DA} in the interval 4.5−5.0 Å are between ∼0.13 eV (eq 4, MN) and ∼0.18 eV (eq 3). Interestingly, more sophisticated calculations based on the Mulliken approximation provided values similar to those obtained using the MN parametrization for γ_{da} integrals.[38]

We can therefore conclude that in contact A2,C1 and A2,C2 ion pairs V_{DA} takes comparable values amounting to not less than ∼1000 cm^{-1}. With reference to Table 2, such a value turns out to be about a half and a third of the respective ΔE_{exc}. Thus, the primary (though not sufficient[10,11]) condition for a Förster-type EET mechanism ($V_{DA} \ll \Delta E_{exc}$) appears to be unfulfilled in either case.

Strictly speaking, the limit of the very weak coupling, when EET may be expected to take place according to eq 5, occurs only at interchromophore distances ≥20 Å (see the next section).

Considering that all the chromophores in Scheme 2 have high S_0-S_1 transition moments, we can expect the other contact ion pairs in Table 2 to feature electronic couplings comparable in the average with those of A2,C1 and A2,C2, except for possible differences due to structural peculiarities.

3.2.3. Dynamic Regime of EET. Using the above calculated donor−acceptor interaction energies, in this section, we will attempt to gain an insight into the EET dynamics with the help of the theory of Kimura et al.[14] outlined in section 3.1.3. For this end, let us consider the three sample ion pairs, (A2,C1), (A2,C2), and (A1,C4), differing from one another in the value of ΔE_{exc} (see Table 2). First of all, the correlation times, τ_c, for the three systems were calculated by eq 11 using the values of τ_r^D, $\mathbf{M}^D$, $\mathbf{M}^A$, and J_{DA} derived from the spectra. Precisely, the transition moments (in debye units) were obtained using the experimental oscillator strengths (f) and transition energies (E_{exc} in cm^{-1}) in the equation $f = 4.68 \times 10^{-7} E_{exc}|\mathbf{M}|^2$. The radiative lifetimes (τ_r) of the anions A1 and A2 acting as excitation energy donors were derived by the Einstein coefficient of spontaneous emission, given by

$$A = \frac{1}{\tau_r^D} = \frac{8\pi^2 \nu_D^3}{3\epsilon_0 \hbar c^3} |\mathbf{M}^D|^2 \qquad (12)$$

TABLE 3: Energies (E_{exc}), Oscillator Strengths (f), and Transition Dipole Moments ($|\mathbf{M}|$) of the $S_0 \rightarrow S_1$ Transition of the Individual Chromophores in Acetonitrile

dye	E_{exc}/cm^{-1}	f	$\lvert\mathbf{M}\rvert$/D	τ_r/ns[a]
A1	21 740	0.83	9.03	3.80
A2	20 830	0.77	8.88	5.68
C1	18 020	1.09	11.37	
C2	17 360	1.70	14.47	
C4	15 360	1.37	13.80	

[a] The radiative lifetimes (τ_r) of the anions A1 and A2 are also given (last column).

where ν_D and $|\mathbf{M}^D|$ are the frequency and the transition dipole moment of the donor S_0-S_1 transition and all quantities need to be expressed in SI units. The so-obtained values of $|\mathbf{M}|$ and τ_r^D are collected in Table 3 together with the starting spectral data.

The spectral overlap integral J_{DA} (M^{-1} cm^3) was then obtained for the three ion pairs by a numerical procedure including: (i) nonlinear multipeak fittings (by means of Gaussian functions), for the absorption spectrum of the acceptor ($\epsilon_A(\lambda)$) and the normalized fluorescence spectrum of the donor ($f_D(\lambda)$) and (ii) numerical integration using both the adaptive Simpson method as well as a higher-order adaptive-recursive method like the one based on Newton−Cotes formulas.

The fitting procedures at point (i) were performed starting from properly selected absorption and emission spectra in dissociating solvents. Briefly, the emission spectra of A2 and A1 were obtained from the emission spectra of A2,C2 in 1:1 propionitrile-butyronitrile and A1,C4 in methanol, respectively. The absorption spectra of C2 (all-trans isomer) and C4 were derived from the fluorescence excitation spectrum of A2,C2 (Figure 3) and the absorption spectrum of A1,C4 in acetonitrile, respectively, while that of C1 was obtained from the absorption spectrum of C1 iodide in acetonitrile. All the spectra were recorded at ordinary temperature. The so-obtained spectral profiles and the corresponding values of J_{DA} are given in Figure 9 stressing the different extent of spectral overlap in the three ion pairs.

From the spectroscopic quantities given in Table 3 and Figure 9, the correlation times τ_c were then calculated by the use of eq 11. They were found to be 15.6, 5.29, and 1.99 fs for (A2,C1), (A2,C2), and (A1,C4), respectively.[46] Using the so-obtained τ_c values, we were finally able to calculate $n_a(t)$, k_{ad}^{max}, and η by eqs 7−10. The analysis was carried out for three values of the electronic coupling (1000, 250, and 40 cm^{-1}) corresponding approximately to equilibrium CIP, 10 Å, and 20 Å distances between the planes of the chromophores. The results concerning the time evolution of the population at the excited state of the acceptor are shown in Figure 10. The comparison between the three panels emphasizes the extent to which the EET dynamics is controlled by the spectral overlap integral J_{DA} (Figure 9), depending in turn on ΔE_{exc} (Table 2). In particular, for V_{DA} = 1000 cm^{-1}, in A2,C1 (curve (a) in the upper panel), $n_a(t)$ exhibits a markedly oscillatory character, with a period of nearly 20 fs, that is indicative of an exciton or partial exciton EET mechanism.[14] The oscillatory character of $n_a(t)$ undergoes a drastic reduction in A2,C2 and vanishes in A1,C4 (curves (a) in the middle and lower panels), thus describing a progressive change from partial exciton to hot-transfer mechanism related to a parallel decrease of J_{DA}. For V_{DA} = 250 cm^{-1}, the $n_a(t)$ curve of A2,C1 ((b) in the upper panel) retains a very weak oscillatory character (emphasized in the inset) revealing a residual partial exciton mechanism. On the other hand, curves (b) in the middle and lower panels both conform to a hot-transfer mechanism,[14]

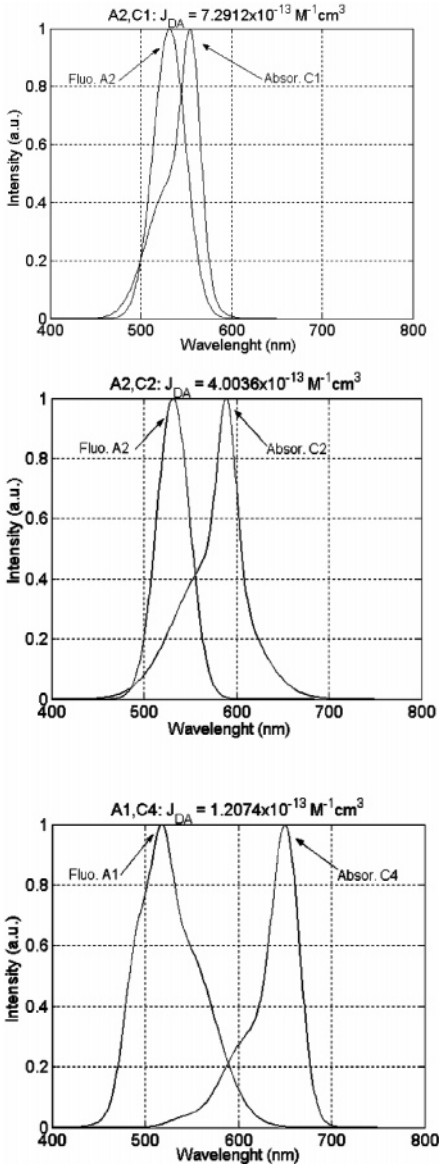

Figure 9. Fluorescence and absorption profiles obtained for (A2,C1), (A2,C2), and (A1,C4) ion pairs by the fitting procedure outlined in the text. The corresponding values of the spectral overlap integral (J_{DA}) are indicated on the top of the three panels.

though as expected the maximum slope decreases sensibly upon moving from A2,C2 to A1,C4. At last, for $V_{DA} = 40$ cm^{-1}, the $n_a(t)$ curve of A2,C1 ((c) in the upper panel) still retains the characteristics of a hot-transfer mechanism. Such characteristics vanish progressively upon moving from A2,C1 to A2,C2 ((c) in the middle panel) and from the latter to A1,C4 ((c) in the lower panel) as emphasized by the insets showing quasi-linear and linear plots near $t = 0$. A fully Förster mechanism is probably reached only in the latter case.

The assignment of the EET dynamic regimes is confirmed by the values of V_{DA} that mark the boundaries of the regions corresponding to the various mechanisms. Such values, calculated according to ref 14, are given in Table 4. As is evident, $V_{DA} = 1000$ cm^{-1} lies in the partial exciton region for both A2,C1 and A2,C2, while it is in the hot-transfer region for A1,C4. $V_{DA} = 250$ cm^{-1} still belongs to the partial exciton region for A2,C1 but falls in the hot-transfer region for both A2,C2 and A1,C4. Finally, $V_{DA} = 40$ cm^{-1} is still within the hot-transfer region for A2,C1, while it is formally in the Förster region for both A2,C2 and A1,C4.

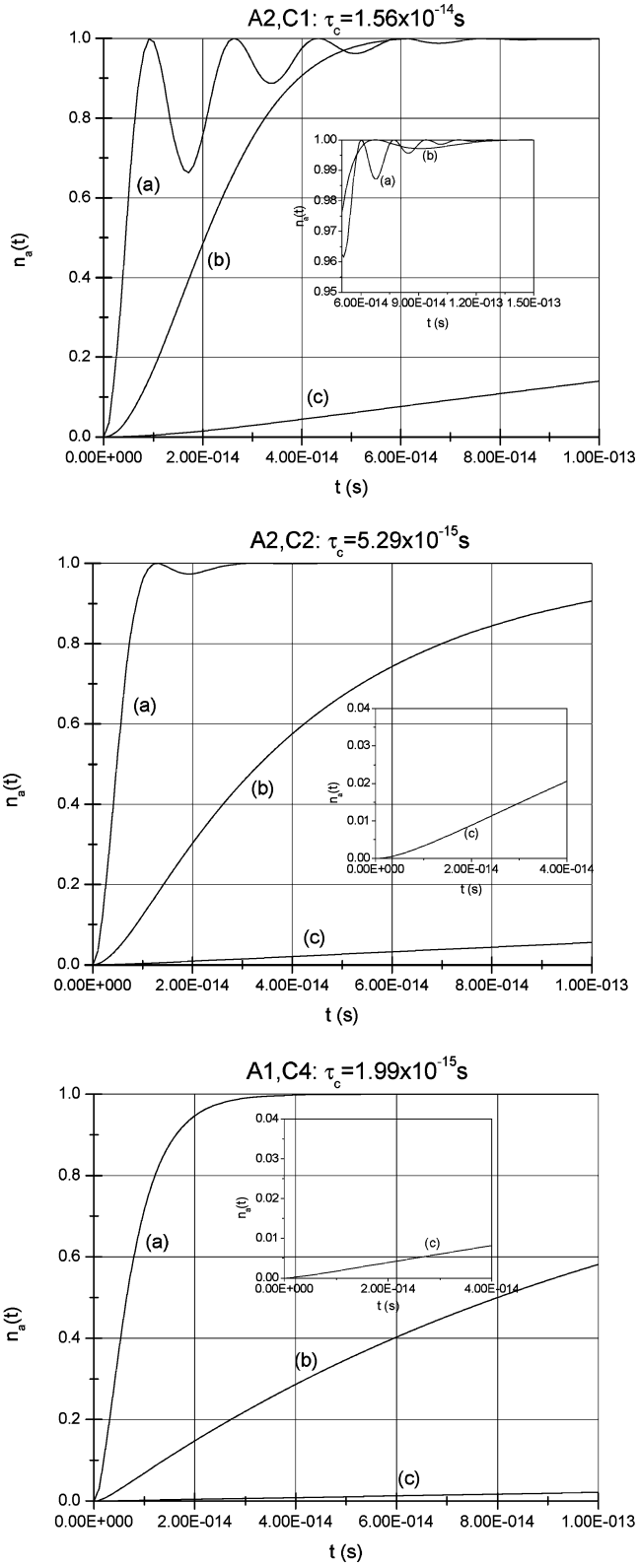

Figure 10. Time dependence of the normalized population at the acceptor excited state for (A2,C1), (A2,C2), and (A1,C4) ion pairs and three values of V_{DA} for each system: 1000 cm^{-1} (a), 250 cm^{-1} (b), and 40 cm^{-1} (c). The τ_c value is indicated on the top of each panel.

Further insight in the EET dynamics of the three ion pairs is provided by the calculated values of k_{ad}^{max} and η collected in Table 5. At the CIP interchromophore separations (i.e., $V_{DA} = 1000$ cm^{-1}), the EET processes in A2,C1 and A2,C2, both lying

TABLE 4: V_{DA} Values (cm^{-1}) Defining the Regions of the Exciton ($V_{DA} > V_{DA}^1$), Partial Exciton ($V_{DA}^3 < V_{DA} < V_{DA}^1$), Hot-Transfer ($V_{DA}^2 < V_{DA} < V_{DA}^3$), and Förster ($V_{DA} < V_{DA}^2$) Mechanisms

ion pair	V_{DA}^1	V_{DA}^3	V_{DA}^2
A2,C1	1082	170	30
A2,C2	3190	501	53
A1,C4	8481	1333	84

TABLE 5: Calculated EET Rate (k_{ad}^{max}) and Coherency (η) for (A2,C1), (A2,C2), and (A1,C4) Ion Pairs at Three V_{DA} Values Representative of the Equilibrium CIP, 10 Å, and 20 Å Interchromophore Separations

	A2,C1		A2,C2		A1,C4	
V_{DA}/cm^{-1}	k_{ad}^{max} (s^{-1})	η	k_{ad}^{max} (s^{-1})	η	k_{ad}^{max} (s^{-1})	η
1000	8.55×10^{13}	0.90	7.11×10^{13}	0.73	4.76×10^{13}	0.43
250	1.66×10^{13}	0.65	9.18×10^{12}	0.30	4.14×10^{12}	0.10
40	8.09×10^{11}	0.13	2.95×10^{11}	0.03	1.13×10^{11}	0.01

in the partial exciton region, have rates not far from 10^{14} s^{-1} and high coherency values. It is to be reminded that in these cases k_{ad}^{max} corresponds to the first maximum slope of the oscillating probability. In A1,C4, k_{ad}^{max} is still above 10^{13} s^{-1} but EET is expected to follow a hot-transfer mechanism, as emphasized by the fact that the coherency is below the critical value ($\eta < \eta_c$). At $R \cong 10$ Å (i.e., $V_{DA} = 250$ cm^{-1}), EET retains partial exciton character in A2,C1 ($\eta > \eta_c$), while it has hot-transfer character in both A2,C2 and A1,C4 (though the latter retains only 10% of the full coherency). Finally, at $R \cong 20$ Å (i.e., $V_{DA} = 40$ cm^{-1}), in A2,C2 and A1,C4 both the values of k_{ad}^{max} ($\sim 10^{11}$ s^{-1}) and the vanishing values of η indicate that a Förster mechanism is virtually reached. On the other hand, despite the large interchromophore separation, in A2,C1, the EET process is found to retain residual hot-transfer character and to take place at the same rate as the vibrational relaxation ($k_{ad}^{max} \approx 10^{12}$ s^{-1}). In summary, the dynamic behavior of EET in the ion pairs under study proves to be fairly describable within the theory proposed by Kimura et al.[14] The results obtained for the CIPs appear to be consistent with the indications provided by steady-state spectroscopy in low-polarity solvents, while those obtained for $R \cong 10$ Å may be tentatively taken as representative of the EET dynamics in SSIPs.

4. Summary and Conclusions

This work is part of a larger study, both experimental and theoretical, on structural, spectroscopic, and photophysical properties of dimers or ion pairs (heterodimers) formed in solutions of ionic cyanine dyes depending on the solvent polarity. Within this subject, we have investigated the problem of the interchromophore EET in ion pairs where an anionic oxonol-like cyanine, acting as an EE donor, is associated with a cationic cyanine, acting as an acceptor. Progressive ion pairing was monitored by electrical conductivity measurements upon moving from highly polar (dissociating) to nonpolar (associating) solvents. While association in ion pairs appears to be almost completed in chloroform, the predominant kind of ion pair is expected to change from SSIP to CIP upon moving from chloroform to toluene. By an analysis of the absorption spectra in chloroform−toluene mixtures with increasing toluene content, we were able to show that the transformation of SSIP into CIP involves fine spectral modifications univocally ascribable to partial exciton resonance taking place in CIPs. Indeed, the size of such an effect proved to be in an inverse order with respect to the ΔE_{exc} of the two chromophores: it was found to decrease in the series A2,C1−A2,C2−A1,C4 according to a corresponding increase of ΔE_{exc} (0.35−0.43−0.79 eV). Clear evidence for the occurrence of interchromophore EET in CIP was gained from fluorescence excitation spectra of A2,C1 and A2,C2 in chloroform−toluene mixtures showing that excitation of the donor (A2) resulted in acceptor (C2 or C1) emission, the intensity of which increased with increasing toluene fraction. Such a trend was confirmed by the values of the EET quantum efficiencies, determined for (A2,C1), (A2,C2), and several other salts in chloroform and chloroform−toluene mixtures. In 9:1 toluene−chloroform mixture, where CIPs are dominant, A1 and A2 anions turned out to be good EE donors toward all the examined cations, with efficiencies ranging from 0.2 to 0.65.

The piece of information obtained by steady-state spectroscopy on the nature and efficiency of EET in the ion pairs under study was complemented by a theoretical investigation aimed at elucidating the dynamic aspects of the EET process in the CIP. The concurrence of high $S_0 \rightarrow S_1$ transition moments and rather short interchromophore distances suggested that, in CIP, EET should deviate to a certain extent from the weak coupling regime where Förster's rate equation can be applied. The quantification of such deviations was attempted within the EET theory developed a few years ago by Kimura, Kakitani, and Yamato for the intermediate coupling case and taking (A2,C1), (A2,C2), and (A1,C4) as sample systems so as to take advantage of the parallel spectroscopic study. Explicit electronic coupling calculations were performed only for A2,C1 and A2,C2. On the basis of MD simulations and local full geometry optimizations, the more probable CIP structures were found to be sandwich-type with 4.5−5.0 Å interchromophore distances (R) and high stabilization energy (~ -210 kJ mol^{-1}). The electronic coupling (V_{DA}), approximated by the Coulombic interaction term, was calculated in terms of atomic transition charges obtained by CS-INDO SCI treatment of the isolated constituent chromophores and using different formulations for the distance dependence of charge−charge interactions. For both A2,C1 and A2,C2, V_{DA} was predicted to be as high as ~ 1000 cm^{-1} at the CIP interchromophore distances and to become ~ 250 cm^{-1} at $R = 10$ Å and ~ 40 cm^{-1} at $R = 20$ Å. These values of V_{DA} were adopted as standard couplings for studying the EET dynamics in (A2,C1), (A2,C2), and (A1,C4). The other basic quantity of the theory τ_c was obtained by a procedure using the spectral data of the isolated chromophores which appear in the Golden-rule rate expression. The value of τ_c, and hence the EET dynamics at a fixed V_{DA}, turned out to be primarily modulated by the spectral overlap integral J_{DA} related in turn to the value of ΔE_{exc}. The theoretical analysis carried out within this scheme led us to the following predictions: (i) at the CIP donor−acceptor separations, the EET dynamics falls within the intermediate coupling case for all of the three sample ion pairs, though the coherent character decreases considerably upon moving from A2,C1 and A2,C2 (where EET takes place with partial exciton mechanism) to A1,C4 (where EET lies in the hot-transfer region), and (ii) at distances as large as $R \cong 20$ Å, the EET mechanism appears to be virtually Förster-type for A2,C2 and A1,C4 (as emphasized by almost vanishing coherency and EET rate of $\sim 10^{11}$ s^{-1}) but retains residual hot-transfer character in A2,C1 where the EET rate is found to be $\sim 10^{12}$ s^{-1}.

Of course, these predictions have qualitative character in consideration of the various assumptions involved in the theoretical description. Thus, real EET dynamics may be overall shifted toward higher or lower coherent character with respect to our prediction which should be subjected to validation by subpicosecond time-resolved spectroscopy.

Acknowledgment. This work was supported by the Grant FIRB RNBE01P4JF from the Italian Ministry of Education and Research (MIUR). Dr. Zh. A. Krasnaya is thanked for providing the dye salts.

Appendix

Evaluation of the EET Efficiency of Non-Emitting Donors. The EET efficiency is usually determined through a comparison of the fluorescence lifetimes and/or quantum yields of the donor in the absence and presence of the acceptor. This approach is, however, obviously limited to systems where the fluorescence intensity of the donor is sufficient for the mentioned comparison. If this is not the case, as in most of our ion pairs, then a steady-state approach based on the fluorescence of the acceptor sensitized by the donor may be useful for evaluating EET efficiencies, provided that some conditions are satisfied.

Under steady-state excitation at wavelength λ, the observed fluorescence emission rate of the acceptor in the ion pair (or, otherwise said, its fluorescence excitation spectrum), $I_f^{DA}(\lambda)$, is given by

$$I_f^{DA}(\lambda) = c[I_{abs}^{A}(\lambda) + I_{abs}^{D}(\lambda) r_{EET}] \quad (1)$$

where c includes instrumental parameters and the acceptor fluorescence quantum yield and spectral shape, $I_{abs}^{A,D}$ are the rates of absorption by the acceptor (A) and the donor (D), and r_{EET} is the efficiency of EET (fraction of excited donor molecules that transfer energy to the partner in the ion pair). If the sample is optically thin, then we approximate $I_{abs}^{A,D} \cong I_{inc}(\lambda) A^{A,D}(\lambda)$, where I_{inc} is the incident light flux and $A^{A,D}$ are the sample absorbances. So

$$I_f^{DA}(\lambda) = c I_{inc}(\lambda)[A^{A}(\lambda) + A^{D}(\lambda) r_{EET}] \quad (2)$$

If the contribution to the observed fluorescence intensity from donor emission is negligible at the monitoring wavelength and at any value of the excitation wavelength, then $I_f^{DA}(\lambda)$ coincides with the measured fluorescence excitation spectrum of the ion pair. The latter can be corrected for the spectral distribution of the excitation source ($I_{inc}(\lambda)$) and the spectral sensitivity curve of the excitation channel ($f_{corr}(\lambda)$) as $I_f'^{DA}(\lambda) = I_f^{DA}(\lambda) f_{corr}(\lambda)/I_{inc}(\lambda)$. This correction introduces a new, arbitrary scale factor. We take it such that the excitation spectrum coincide with the absorption spectrum in the region of the acceptor band (in the cases of salts with the C2 and C2(Et) cations, where, as previously described, cis−trans isomer equilibrium complicates the absorption spectra, the scale factor was taken so that the red side of the excitation spectrum matched the red side of the absorption spectrum). Therefore, under these normalized scales

$$I_f'^{DA}(\lambda) = A^{A}(\lambda) + A^{D}(\lambda) r_{EET} \quad (3)$$

Thus, from a comparison of the absorption and the corrected fluorescence excitation spectra of the ion pair, an evaluation of r_{EET} as a function of the excitation wavelength can be obtained. In particular, if the acceptor has a negligible absorption in the region of the donor band (λ_D), then

$$r_{EET} = I_f'^{DA}(\lambda_D)/A^{D}(\lambda_D) \quad (4)$$

Otherwise, we shall need to obtain the absorption band of the acceptor with a non-chromophoric partner in the same solvent and calculate the energy-transfer efficiency as

$$r_{EET} = [I_f'^{DA}(\lambda_D) - A^{A}(\lambda_D)]/[A^{D}(\lambda_D) - A^{A}(\lambda_D)] \quad (5)$$

References and Notes

(1) Mishra, A.; Behera, R. K.; Behera, P. K.; Mishra, B. K.; Behera, G. B. *Chem. Rev.* **2000**, *100*, 1973.

(2) Möbius, D. *Adv. Mater.* **1995**, *7*, 437. Ikegami, K.; Mingotaud, C.; Lan, M. *J. Phys. Chem. B* **1999**, *103*, 11261.

(3) Fukumoto, H.; Yonezawa, Y. *Thin Solid Films* **1998**, *327*−*329*, 748.

(4) Baraldi, I.; Momicchioli, F.; Ponterini, G.; Tatikolov, A. S.; Vanossi, D. *Phys. Chem. Chem. Phys.* **2003**, *5*, 979.

(5) Baraldi, I.; Caselli, M.; Momicchioli, F.; Ponterini, G.; Vanossi, D. *Chem. Phys.* **2002**, *275*, 149.

(6) Caselli, M.; Latterini, L.; Ponterini, G. *Phys. Chem. Chem. Phys.* **2004**, *6*, 3857.

(7) Baraldi, I.; Momicchioli, F.; Ponterini, G.; Tatikolov, A. S.; Vanossi, D. *J. Phys. Chem. A* **2001**, *105*, 4600.

(8) Davydov, A. S. *Theory of Molecular Excitons*; Plenum Press: New York, 1971.

(9) Kasha, M.; Rawls, H. R.; El-Bayoumi, M. *Pure Appl. Chem.* **1966**, *11*, 371.

(10) Förster, T. Delocalized Excitation and Excitation Transfer. In *Modern Quantum Chemistry, Part III*; Sinanoglu, O., Ed.; Academic Press: New York, 1965.

(11) Valeur, B. *Molecular Fluorescence*; *Principles and Applications*; Wiley-VCH Verlag GmbH: Berlin, 2001; chapter 4.

(12) Volkhard, M.; Kühn, O. *Charge and Energy Transfer Dynamics in Molecular Systems*; Wiley-VCH Verlag GmbH: Berlin, 2000.

(13) Kakitani, T.; Kimura, A.; Sumi, H. *J. Phys. Chem. B* **1999**, *103*, 3720.

(14) Kimura, A.; Kakitani, T.; Yamato, T. *J. Phys. Chem. B* **2000**, *104*, 9276.

(15) HyperChem. *Computational Chemistry Manual*; Hypercube, Inc.; Gainesville, FL, 1996.

(16) Stewart, J. J. P. *J. Comput. Chem.* **1989**, *10*, 221.

(17) Momicchioli, F.; Baraldi, I.; Bruni, M. C. *Chem. Phys.* **1983**, *82*, 229.

(18) Ecoffet, C.; Markovitsi, D.; Millié, P.; Lemaistre, J.-P. *Chem. Phys.* **1993**, *177*, 629.

(19) Markovitsi, D.; Germain, A.; Millié, P.; Lécuyer, P.; Gallos, L.; Argyrakis, P.; Bengs, H.; Ringsdorf, H. *J. Phys. Chem.* **1995**, *99*, 1005.

(20) Marguet, S.; Markovitsi, D.; Millié, P.; Sigal, H.; Kumar, S. *J. Phys. Chem.* **1998**, *102*, 4697.

(21) Millié, P.; Momicchioli, F.; Vanossi, D. *J. Phys. Chem. B* **2000**, *104*, 9621.

(22) Scholes, G. D.; Ghiggino, K. P. *J. Chem. Phys.* **1994**, *101*, 1251.

(23) Bockman, T. M.; Kochi, J. K. *J. Am. Chem. Soc.* **1989**, *111*, 4669.

(24) Hogen-Esch, T. E. In *Advances in Physical Organic Chemistry*; Gold, V., Bethell, D., Eds.; Academic Press: London, 1977; Vol. 15, p 153.

(25) Berkowitz, M.; Karim, O. A.; McCammon, J. A.; Rossky, P. J. *Chem. Phys. Lett.* **1984**, *105*, 577.

(26) Ciccotti, G.; Ferrario, M.; Hynes, J. T.; Kapral, R. *Chem. Phys.* **1989**, 129, 241.

(27) Rey, R.; Guardia, E. *J. Phys. Chem.* **1992**, *96*, 4712.

(28) Smith, D. E.; Dang, L. X. *J. Chem. Phys.* **1994**, *100*, 3757.

(29) Madhusoodanan, M.; Tembe, B. L. *J. Phys. Chem.* **1995**, 99, 44.

(30) Hogen-Esch, T. E.; Smid, J. *J. Am. Chem. Soc.* **1966**, *88*, 307.

(31) Soumillion, J. Ph.; Vandereecken, P.; Van Der Auweraer, M. F.; De Schryver, C.; Schanck, A. *J. Am. Chem. Soc.* **1989**, *111*, 2217.

(32) Brooker, L. G. S.; Heseltine, D. W.; Lincoln, L. L. *Chimia* **1966**, *20*, 327.

(33) West, W.; Pearce, S.; Grum, F. *J. Phys. Chem.* **1967**, *71*, 1316.

(34) Vranken, N.; Jordens, S.; De Belder, G.; Lor, M.; Rousseau, E.; Schweitzer, G.; Toppet, S.; Van der Auweraer, M.; De Schryver, F. C. *J. Phys. Chem. A* **2001**, *105*, 10196.

(35) Baraldi, I.; Carnevali, A.; Momicchioli, F.; Ponterini, G. *Spectrochim. Acta, Part A* **1993**, *49*, 471.

(36) Scholes, G. D.; Ghiggino, K. P. *J. Phys. Chem.* **1994**, *98*, 4580.

(37) Scholes, G. D. Theory of coupling in multichromophoric systems. In *Resonance Energy Transfer*; Andrews, D. L., Demidov, A. A., Eds.; Wiley: Chichester, U.K., 1999; Chapter 6, p 212.

(38) Baraldi, I.; Fiorini, M.; Vanossi, D. To be submitted for publication.

(39) Beljonne, D.; Cornil, J.; Silbey, R.; Millié, P.; Brédas, J. L. *J. Chem. Phys.* **2000**, *112*, 4749.

(40) Ohno, K. *Theor. Chim. Acta* **1964**, *2*, 219. Klopman, G. *J. Am. Chem. Soc.* **1964**, *86*, 4550.

(41) Mataga, N.; Nishimoto, K. *Z. Physik. Chem.* **1957**, *12*, 335; **1957**, *13*, 140.

(42) When V_{DA} is approximated by the dipole−dipole interaction between the transition dipole moments $|\mathbf{M}^{D}|$ and $|\mathbf{M}^{A}|$, eq 5 reduces to the usual Förster equation.[10]

(43) Cho, M.; Silbey, R. J. *J. Chem. Phys.* **1995**, *103*, 595.

(44) Equation 7 was derived[14] neglecting the (generally weak) time dependence of the correlation time, and taking $\tau_c(t_1) = \tau_c(0)$. Here, $\tau_c(0)$ is abbreviated at τ_c.

(45) See eqs 55−58 and Appendix D in ref 14.

(46) We note that, considering the very short values of τ_c the spectral overlap J_{DA} should be calculated using the emission spectrum from the Franck−Condon state that is somewhat blue shifted from the steady-state fluorescence spectrum. Thus, the use of the fluorescence spectrum involves underestimation of the peak separation between the emission spectrum of the donor and the absorption spectrum of the acceptor, and hence it may lead to a certain overestimation of J_{DA}.